A piezoresistive micro-cantilever for thermal infrared detector

Jintao Liang (梁晋涛)[1], Junhua Liu (刘君华)[1], Xin Li (李 昕)[2], and Changchun Zhu (朱长纯)[2]

[1] *School of Electrical Engineering, Xi'an Jiaotong University, Xi'an 710049*
[2] *School of Electronics and Information Engineering, Xi'an Jiaotong University, Xi'an 710049*

Received June 8, 2005

A novel tri-layer Si-based micro-cantilever thermal infrared (IR) detector with carbon nanotube (CNT) film is fabricated. It is based on the characteristic that the composite micro-cantilever bends in response to incident IR thermal radiation due to the bi-material effect. The bending of micro-cantilever is piezoresistively detected. Furthermore, a new IR absorbing layer material — CNTs — is coated in order to enhance IR radiation absorbing characteristic. the micro-electro-mechanical system (MEMS) sensor could be compatible with integrated circuit technology.

OCIS codes: 040.0040, 120.0120, 310.0310.

Recently, there has been an increasing interest in the development of uncooled infrared (IR) thermal detector using composite micro-cantilevers because of their advantages such as low cost, low weight, low power, wide spectral response, and long-term operation compared with photon detectors[1−4]. The composite micro-cantilever detectors bend in response to incident IR radiation due to the bi-material effect[5,6]. In a thermal detector, the incident radiation is absorbed so that the material temperature is changed. In a bi-material structure, the lengths of the two layers change by different thermal expansion coefficients of coating and substrate materials and the resulted stress causes the structure to bend. Presently, the IR thermal detector consists of a silicon or silicon nitride cantilever and a coating of aluminum or gold on one side[6−9]. In such a bi-layer micro-cantilever thermal IR detector, the metallic coating film shows a low absorption coefficient for the incoming radiation. To overcome the difficulty, we design a novel tri-layer micro-cantilever thermal IR detector, which can be fabricated using standard semiconductor and micro-mechanical process technology. The micro-cantilever bending due to IR absorption is observed by a piezoresistive technique. Carbon nanotube (CNT) film is used as the third layer to enhance the IR absorbing characteristic.

The micro-cantilever IR thermal detector consisted of a Si/Al/CNT tri-layer structure as shown in Fig. 1. The micro-cantilever was rectangular and its dimension was 1000 μm in length and 100 μm in width. The silicon layer was 15 μm in thickness and the aluminum layer was 1 μm in thickness. Implanted p-type silicon resistors were used for piezoresistive detection (close to the root of the cantilever) of micro-cantilever bending. Aluminum lines were used for electrical connection. Thermal evaporation was used to deposit 1-μm-thick film of aluminum on the back of silicon. The surface of aluminum layer was smeared with CNTs slurry (Fig. 2). The sol in the CNTs was evaporated at 300 °C. The micro-cantilever chip was bonded with a glass encapsulation by electrostatic bonding.

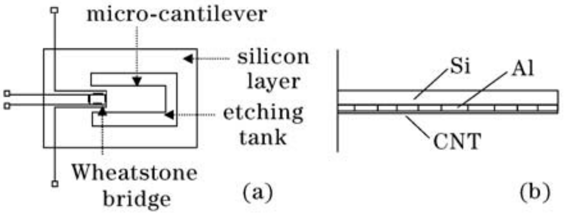

Fig. 1. The top view (a) and cross-section (b) of the micro-cantilever detector.

The piezoresistive sensitivity of rectangular cantilever beam is

$$\frac{\Delta R}{R} = \pi_{\mathrm{L}}\sigma_{\mathrm{L}} + \pi_{\mathrm{T}}\sigma_{\mathrm{T}}, \tag{1}$$

where R is the resistance of piezoresistor, ΔR is the resistance change, π_{L} and π_{T} are defined as the longitudinal and transverse piezoresistance coefficients, σ_{L} and σ_{T} are the longitudinal and transverse components of the stress σ, respectively.

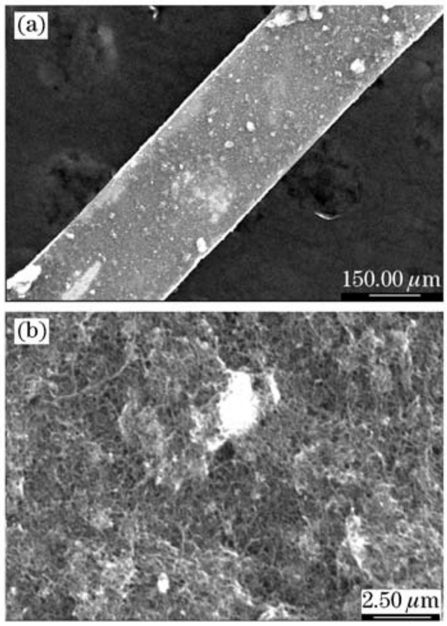

Fig. 2. SEM photos of the surface of micro-cantilever with CNT (a) and the surface of CNT film (b).

1671-7694/2006/030128-03 http://www.col.org.cn

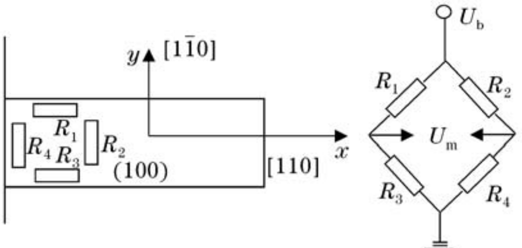

(a) (b)

Fig. 3. (a) Silicon cantilever with piezoresistor; (b) Wheatstone bridge configuration of the four piezoresistive elements.

The values of π_L and π_T depend on several properties of the crystal, and on the orientation of the stress σ related to the crystal lattice orientation of the single crystal silicon. As shown in Fig. 3(a), for a (100) oriented silicon wafer, the piezoresistive coefficients for silicon with low doping concentration vary as a function of direction. For p-type silicon, the piezoresistive coefficients are largest along $\langle 110\rangle$ directions. π_L and π_T are

$$\pi_L = \frac{1}{2}\pi_{44}, \quad \pi_T = -\frac{1}{2}\pi_{44}, \tag{2}$$

where π_{44} is shear piezoresistance coefficient. The micro-cantilever bends in response to incident IR radiation due to the bi-material effect. As the temperature of the bi-material structure changes, the lengths of the two layers change by different amounts and the resulted stress causes the structure to bend. Based on the beam deflection theory, the maximum stress σ is at the base of the beam and is longitudinal.

$$\sigma_L = \sigma_x, \quad \sigma_T = \sigma_y = 0, \quad \sigma_x = \frac{6lk}{wt^2}\Delta z, \tag{3}$$

where l is the length of cantilever beam, w is the width of cantilever beam, t is the thickness of cantilever beam, k is the spring constant of cantilever beam, and Δz is the displacement of cantilever beam end. The stress in a rectangular beam cantilever consisting of two materials with different thermal expansion coefficients induces a bending Δz given by[10]

$$\Delta z = \frac{l^2}{t}\left(\frac{(1+x)^2(\alpha_1-\alpha_2)}{3(1+x)^2+(1+xn)(x^2+\frac{1}{xn})}\right)\Delta T, \tag{4}$$

n and x are defined by

$$n = \frac{E_1}{E_2}, \quad x = \frac{t_1}{t_2}, \tag{5}$$

where E_1 and E_2 stand for the Young's modulus of the micro-cantilever coating (Al) and the substrate (Si), respectively, and t_1 is the Al coating thickness, t_2 is the Si substrate thickness, α_1 and α_2 are the thermal expansion coefficients of the Al and Si, respectively, ΔT is the temperature change of the micro-cantilever.

Figure 3(a) shows the top view of an arrangement of four piezoresistors aligned with the base oriented along the $\langle 110\rangle$ silicon lattice direction. Figure 3(b) shows Wheatstone bridge configuration of the four piezoresistive elements. Due to the piezoresistors' orientations, their resistance R_1 and R_3 will increase, R_2 and R_4 will decrease,

$$\frac{\Delta R_1}{R_1} = \frac{\Delta R_3}{R_3} = \pi_L\sigma_x, \quad \frac{\Delta R_2}{R_2} = \frac{\Delta R_4}{R_4} = \pi_T\sigma_x, \tag{6}$$

where

$$R_1 = R_2 = R_3 = R_4 = R. \tag{7}$$

For p-type resistors, the relative increases in R_1 and R_3 are equal to the relative decreases in R_2 and R_4. If all resistors have the same unstressed resistance value, then a simple circuit analysis of the Wheatstone bridge configuration shows that two voltages U_b (the outer voltage bias) and U_m (the output measured voltage) determine $\Delta R/R$ by

$$\begin{aligned}\frac{\Delta R}{R} &= \frac{U_m}{U_b} \\ &= \pi_{44}\frac{6l^3k}{wt^3}\left(\frac{(1+x)^2(\alpha_1-\alpha_2)}{3(1+x)^2+(1+xn)(x^2+\frac{1}{xn})}\right)\Delta T. \end{aligned}\tag{8}$$

The incident IR radiation intensity can be measured from the measurement of the temperature change of the micro-cantilever, because this charge leads to stress which causes the bi-material structure to bend. The bending of micro-cantilever is piezoresistively detected. To effectively transform IR radiation into heat, the micro-cantilever is covered with an absorbing layer. To achieve high sensitivity, the absorption must be high. The most effective mechanism for light absorption is high porosity. Particles with sizes much smaller than light wavelength generally absorb and diffract the light. The absorption streches over the whole spectral range. On the other hand, in order not to increase the time constant of the sensor, the mass of the layer has to be small[11]. CNTs have high specific surface area and highly porous structure[12], so it is suitable to use CNTs as the absorbing layer to cover the composite micro-cantilever.

The input-output characteristic of the piezoresistive micro-cantilever IR thermal detector was experimentally studied. The experimental diagram is shown in Fig. 4. U_s was the input IR radiation source control voltage (TH-SS305), the higher the input voltage U_s, the larger the IR radiation power. The incident IR radiation was reflected and collimated by the holophote (TR45) and collimator tube (ACM-200-38) and then irradiated the micro-cantilever. The piezoresistive micro-cantilever measured the incident IR radiation intensity via the temperature change of the micro-cantilever. The output was the Wheatstone bridge voltage U_m (TH-V_1). The input-

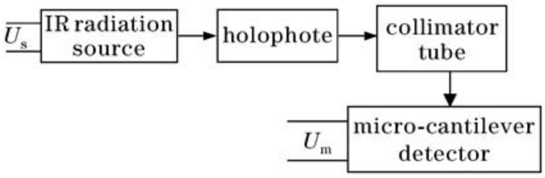

Fig. 4. Experimental diagram for the input-output characteristic of the tri-layer IR thermal detector.

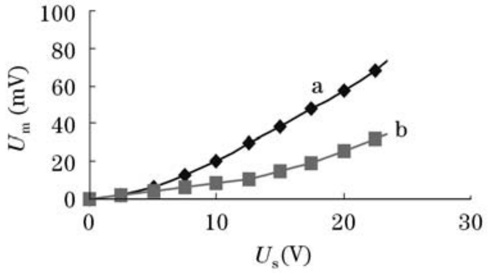

Fig. 5. Input-output characteristic of the tri-layer (a) and bi-layer (b) micro-cantilever IR thermal detectors.

output characteristic is the relationship between the control voltage of IR radiation source and the output Wheatstone bridge voltage U_{m}. Figure 5 depicts the input-output voltages of the tri-layer (Si/Al/CNT) micro-cantilever detector with CNTs absorbing layer (curve a) and of the bi-layer (Si/Al) micro-cantilever detector (curve b). The experimental result shows that higher sensitivity can be achieved by using the micro-mechanical cantilever with CNT absorbing layer. The power resolution ($U_{\mathrm{m}}/U_{\mathrm{s}}$) is increased twice.

A new tri-layer piezoresistive micro-cantilever thermal IR detector with CNT film is successfully fabricated. By using the CNT film and Wheatstone bridge configuration, higher sensitivity in comparison with the bi-layer micro-cantilever detector can be achieved.

This work was jointly supported by the National Natural Science Foundation of China under Grant No. 60276037. J. Liang's e-mail address is dxljt@163.com.

References

1. L. R. Senesac, J. L. Corbeil, S. Rajic, N. V. Lavrik, and P. G. Datskos, Ultramicroscopy **97,** 451 (2003).
2. J.-K. Kim and C.-H. Han, Sensors and Actuators A **89,** 22 (2001).
3. A. Vidic, D. Then, and Ch. Ziegler, Ultramicroscopy **97,** 407 (2003).
4. A. Rogalski, Infrared Phys. Technol. **43,** 187 (2002).
5. J. Yang, T. Ono, and M. Esashi, Sensors and Actuators A **82,** 102 (2000).
6. W. Fang, H.-C. Tsai, and C.-Y. Lo, Sensors and Actuators A **77,** 21 (1999).
7. H. Li, B. Huang, D. Yi, H. Cui, Y. He, and J. Peng, Chin. Opt. Lett. **2,** 171 (2004).
8. X. Chen, Z. Jing, S. Sun, and G. Xiao, Chin. Opt. Lett. **2,** 694 (2004).
9. H. Hu, Z. Jing, and S. Hu, Chin. Opt. Lett. **3,** 322 (2004).
10. O. Nakabeppu, M. Chandrachood, Y. Wu, J. Lai, and A. Majumdar, Appl. Phys. Lett. **66,** 694 (1995).
11. W. Lang, K. Kühl, and H. Sandmaier, Sensors and Actuators A **34,** 243 (1992).
12. Y.-F. Liu, Z.-M. Shen, Y. Kiyoshi, B.-H. Ma, and J.-M. Yu, New Carbon Materials (in Chinese) **19,** 197 (2004).